

Power Line Network Topology Inference Using Frequency Domain Reflectometry

Mohamed Osama Ahmed and Lutz Lampe

Department of Electrical and Computer Engineering, University of British Columbia, Vancouver, Canada
 {mohameda, lampe}@ece.ubc.ca

Abstract—Frequency Domain Reflectometry (FDR) is a technique that was proposed for fault detection in Digital Subscriber Line (DSL) cables. In this paper, we describe how FDR can be used to determine the topology of power line networks. To this end, we first infer distance information from the multiple signal reflections measured and processed with FDR. Then, we present an algorithm that uses these distance measurements to reconstruct the topology step by step operating on a network graph. Numerical results for sets of sample networks demonstrate the effectiveness of the proposed topology-inference approach.

I. INTRODUCTION

Power line communications (PLC) is an attractive technology for data communication as it reuses an existing infrastructure. Its origins go back to the early 1900's, and it has long been used for control and automation by electricity utilities, cf. [1, Ch. 1]. PLC has gained broader attention through its application for Internet access and multimedia streaming. More recently, PLC is considered as one of the technologies suitable to enable Smart Grid concepts, e.g., [2], [3]. Both application areas have stimulated renewed research and development efforts, which also led to the introduction of modern communications concepts to PLC, such as cooperative communication, multiple-input multiple-output (MIMO) transmission, advanced routing, etc., cf. e.g. [2], [4]–[9]. To validate these algorithms, PLC network configurations are needed. One approach to generate these is based on statistical assumptions about branch lengths and number of nodes in networks, e.g. [5], [10]. In the context of Smart Grid, often simplifying or ad-hoc assumptions are made, since topologies of realistic configurations are not well studied, e.g., [2], [6], [9]. In fact, electricity utilities often have incomplete and inaccurate information about the details of their power line infrastructure and would be interested in updated information based on in-situ measurements.

In this paper, we ask the question of how to infer the topology of PLC networks. That is, given a power line infrastructure, we are interested in the location of branches and loads. Since PLC operates on this infrastructure, this determines the PLC network topology. Thus, the application of this inference provides instances of realistic PLC topologies. Another use of this method is for diagnostics of the power grid or optimization of distributed energy sources in micro

grids, which benefits from knowledge of physical distances between network nodes [11]. We are interested in a solution that performs measurements at one or a few points of the grid to obtain topology information. Thereby, we are inspired by approaches in the DSL domain, which apply time-domain reflectometry (TDR) and frequency-domain reflectometry (FDR) for fault detection in cables, e.g. [12], [13].

This paper is organized as follows. Section II reviews some basic parameters of transmission line theory and FDR principles applied in this work. Then, Section III describes how we can use FDR for PLC topology inference, leading to the proposed algorithm. Simulation results for a number of test topologies are presented in Section IV for some examples, and conclusions are given in Section V.

II. PRELIMINARIES

A. Transmission Line Model

In this paper, we are going to use the two-conductor transmission line model for describing signal propagation over power lines [1, Ch. 2]. The transmission line is described by its primary parameters R , G , L , and C , which represent the resistance, conductance, inductance and capacitance per unit length, respectively. These parameters can be calculated for different types of cables. In general, they are functions of the frequency f . The characteristic impedance Z_0 and the complex propagation constant γ represent the secondary parameters of the transmission line. Z_0 is calculated by

$$Z_0 = \sqrt{(R + j2\pi fL)/(G + j2\pi fC)} \quad (1)$$

and γ is given by

$$\gamma = \sqrt{(R + j2\pi fL)(G + j2\pi fC)}. \quad (2)$$

We can write $\gamma = \alpha + j\beta$, where α and β are the attenuation and the propagation constants, respectively. These parameters determine how the wave propagates through the line (i.e. the magnitude and the phase of the voltage signal).

B. FDR Review

FDR has been proposed as an alternative to TDR for detection of different types of cable faults in DSL, cf. e.g. [13]–[17]. Following the description in [15], in FDR a sinusoidal signal of frequency f is injected and propagates through the line as

$$V_t(x, t) = Ae^{-\alpha x} \cos(2\pi ft - \beta x), \quad (3)$$

where $V_t(x, t)$ represents the voltage of the transmitted signal as a function of the travel distance x and time t , and A is the amplitude of the transmitted signal.¹ Whenever the transmitted signal encounters a discontinuity, it is reflected. The reflection coefficient Γ can be calculated by

$$\Gamma = \frac{Z - Z_0}{Z + Z_0} = |\Gamma| e^{j\angle\Gamma}, \quad (4)$$

where Z is the impedance seen at the discontinuity and $|\Gamma|$ and $\angle\Gamma$ represent the magnitude and the phase of the reflection coefficient at the point of discontinuity, respectively. The voltage of the reflected signal $V_r(x, t)$ is described by

$$V_r(x, t) = A |\Gamma| e^{-\alpha(2\ell-x)} \cos(2\pi ft - \beta(2\ell - x) + \angle\Gamma), \quad (5)$$

where ℓ is the distance from the point of measurement to the point where the reflection took place (the location of the discontinuity), so that the round trip distance is 2ℓ . As can be seen from (5), the magnitude of the reflected signal is changed by a factor $|\Gamma|$, and its phase is shifted by $\angle\Gamma$. The measured reflected signal $V_r(0, t)$ is then correlated with the transmitted signal $V_t(0, t)$ and passed through a low pass filter (LPF) for coherent demodulation. The output of LPF, $Y(f)$, is called the trace. It can be written as

$$Y(f) = \frac{A}{2} |\Gamma| e^{-2\alpha\ell} \cos(2\beta\ell - \angle\Gamma). \quad (6)$$

The trace is measured for a certain frequency range (from a minimum frequency f_{\min} to a maximum frequency f_{\max}), with a certain step size Δf . In case of low losses, β can be approximated as $\beta = 2\pi f\sqrt{LC}$, and thus the propagation speed is $v = \frac{1}{\sqrt{LC}}$. The trace $Y(f)$ can then be expressed as

$$Y(f) = \frac{A}{2} |\Gamma| e^{-2\alpha\ell} \cos(4\pi f\sqrt{LC}\ell - \angle\Gamma). \quad (7)$$

By taking the Inverse Fourier Transform (IFT) of (7), the signal is transformed to the "correlation" $y(t)$ in the time domain. $y(t)$ will have a peak at $t = 2\sqrt{LC}\ell$, and thus the location of the discontinuity can be determined at $d = vt = 2\ell$.

For (7), we assumed the low-losses case to simplify the analysis only. If it is not satisfied, then the analysis can be extended to the general case by rescaling the frequency axis properly as discussed in [15]. Likewise, the possible frequency-dependency of α can be compensated for, typically with a high-pass filter. If the reflection coefficient Γ is a function of frequency, and the dependency of α on f is not compensated for (since it may not be known a priori), then the peaks in $y(t)$ will be broadened, which is the spectral leakage problem. This limits the resolution of multiple peaks and requires the application of windowing.

In fact, since the measurement frequency range is finite (from f_{\min} to f_{\max}), $Y(f)$ from (7) can be thought of as being multiplied with a rectangle function and thus there is a minimum distance Δd_{\min} between two reflection points that can be detected. Applying windowing helps in suppressing sidelobes

¹In (3) we did not make the frequency-dependence of α and β explicit, but we will comment on it in the following.

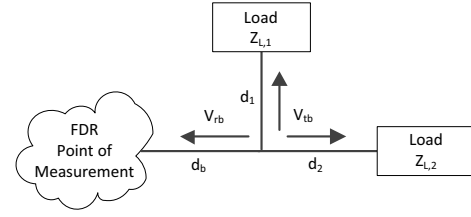


Fig. 1. Topology with 2 loads and 1 branch point.

of peaks. The resolution can be approximated according to the relation

$$\Delta d_{\min} \propto \frac{1}{(f_{\max} - f_{\min})\sqrt{LC}}. \quad (8)$$

III. FDR FOR PLC TOPOLOGY DETECTION

Consider the simple topology shown in Fig. 1 consisting of one branch point and two loads. The transmitted signal propagates through the line till it reaches the branch point, where part of the signal is reflected, denoted by V_{rb} , and the other part V_{tb} is transmitted. At the branch point we have

$$V_{rb}(d_b, t) = A |\Gamma_b| e^{-\alpha d_b} \cos(2\pi ft - \beta d_b + \angle\Gamma_b) \quad (9)$$

and

$$V_{tb}(d_b, t) = A |T_b| e^{-\alpha d_b} \cos(2\pi ft - \beta d_b + \angle T_b). \quad (10)$$

Γ_b and T_b are, respectively, the reflection and the transmission coefficients at the branch point from the source's side. The transmitted signal is then reflected from the first and the second loads. The trace $Y(f)$ will be a summation of the reflected signals. The first three terms are given by

- (i) $A |\Gamma_b| e^{-2\alpha d_b} \cos(2\beta d_b - \angle\Gamma_b)$
- (ii) $A |T_b| |\Gamma_{L,1}| |T_{b,1}| e^{-2\alpha(d_b+d_1)} \times \cos(2\beta(d_b+d_1) - \angle\Gamma_{L,1} - \angle T_b - \angle T_{b,1})$ (11)
- (iii) $A |T_b| |\Gamma_{L,2}| |T_{b,2}| e^{-2\alpha(d_b+d_2)} \times \cos(2\beta(d_b+d_2) - \angle\Gamma_{L,2} - \angle T_b - \angle T_{b,2})$

The first term represents the reflection from the branch point, while the second and the third terms represent the reflection from the first and the second load with reflection coefficients $\Gamma_{L,1}$ and $\Gamma_{L,2}$, respectively. $T_{b,1}$ and $T_{b,2}$ are the transmission coefficients at the branch point from the first and second load's side, respectively. We note that transmission and reflection coefficients are related by

$$T = 1 + \Gamma. \quad (12)$$

The reflection coefficient from the branch Γ_b is independent of the loads. It only depends on the characteristic impedances of the transmission lines. Assuming that all the branches have the same characteristic impedance Z_0 , the equivalent impedance at the branch point is given by $Z_b = Z_0/N_b$, where N_b is the number of branches at the branch point. Then, the reflection coefficient becomes

$$\Gamma_b = \frac{Z_b - Z_0}{Z_b + Z_0} = \frac{1 - N_b}{1 + N_b}, \quad (13)$$

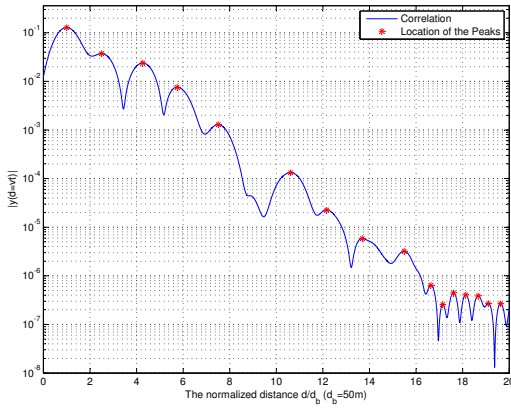


Fig. 2. Correlation $y(d = vt)$ of the trace $Y(f)$ of the sample topology from Fig. 1.

and the angle of the reflection coefficient for the branch point is $\angle\Gamma_b = \pi$. Since also the angle of the transmission coefficient is 0, the formula for the trace $Y(f)$ simplifies significantly. In particular, the first three terms from (11) simplify to

$$\begin{aligned}
 & \text{(i)} \quad -A |\Gamma_b| e^{-2\alpha d_b} \cos(2\beta d_b) \\
 & \text{(ii)} \quad A |T_b| |\Gamma_{L,1}| |T_{b,1}| e^{-2\alpha(d_b+d_1)} \\
 & \quad \times \cos(2\beta(d_b+d_1) - \angle\Gamma_{L,1}) \\
 & \text{(iii)} \quad A |T_b| |\Gamma_{L,2}| |T_{b,2}| e^{-2\alpha(d_b+d_2)} \\
 & \quad \times \cos(2\beta(d_b+d_2) - \angle\Gamma_{L,2})
 \end{aligned} \tag{14}$$

The expressions in (14) show that the magnitude and the phase of the FDR measurements can be used to determine the location of branches and loads as well as the value of the load impedances. However, it is important to note that for this method to work, we need the following conditions:

- 1) α and β are known over the measurement frequency range.
- 2) Load impedances are constant over the frequency range of the measurement.
- 3) Characteristic impedances of the cables in the network are identical.

Since these conditions are not always satisfied in practical cases, in the following we propose an algorithm that uses only the distance measurements from FDR to determine the topology of the power line network.

To this end, consider the correlation $y(d = vt)$ in Fig. 2 for the trace $Y(f)$ of the sample topology from Fig. 1. The correlation was generated using $f_{\min} = 50$ kHz, $f_{\max} = 3$ MHz, $\Delta f = 1$ kHz, transmission line parameters as described in [1, Ch. 2.3] for NAYY150SE power line cables, and Blackman windowing. The distances are $d_b = 50$ m, $d_1 = 75$ m, and $d_2 = 162.5$ m, the load impedances were chosen as $Z_{L,1} = 36e^{j0.09} \Omega$ and $Z_{L,2} = 26e^{j0.36} \Omega$. We observe the broadening of the correlation peaks due to realistic transmission line parameters and finite measurement bandwidth. The red markers show the peaks, whose locations correspond to

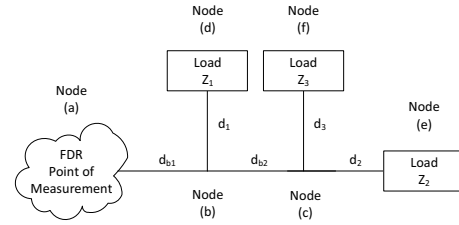


Fig. 3. Example of a PLC network.

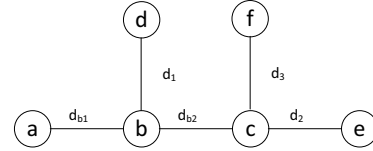


Fig. 4. Graph representation of the topology in Fig. 3.

the distance traveled by signals. These locations will be used in the following.

A. Ideal FDR Spectrum

Using the peak locations of the correlation $y(d)$ only allows us to tackle the problem of topology inference from a more abstract level. Let us consider the somewhat larger power line topology shown in Fig. 3. We model this topology as a graph with branch points and loads being the vertices and the power lines being the edges. Figure 4 shows the corresponding graph. For the graph in Fig. 4, the “ideal” FDR correlation can be generated by considering all the possible walks in the graph that start from and end in node ‘a’. It is important to note that a walk can include the same node or the same edge more than once as for example the walk a-b-d-b-d-b-a. Figure 5 shows the ideal FDR correlation. Since we are interested in the distance only, the magnitude and phase of $y(d)$ is ignored, and thus all arrows in Fig. 5 have the same height. The ideal FDR correlation can be expressed as ($\delta(x)$ is the Delta impulse)

$$y(d) = \delta(d - 2(d_{b1} + id_1 + jd_{b2} + kd_2 + ld_3)) \tag{15}$$

for all non-negative integers i, j, k , and ℓ , under the condition that $k = \ell = 0$ if $j = 0$, since we cannot add nodes ‘e’ and ‘f’ without walking the branch b-c first.

B. Limiting the Number of Echoes Per Branch

The case of the ideal correlation includes infinite number of reflections. In order to have a stopping criterion for the algorithm, which will be explained below, we limit the number of reflections per branch to a maximum number. For example if the maximum number of echoes per branch is 3, then the walk (a-b-d-b-d-b-d-b-a) is not allowed because the signal is reflected 4 times through the branch b-d, while the cycle (a-b-d-b-d-b-a) is allowed. This assumption is realistic since at each signal reflection the magnitude of the voltage is multiplied by reflection coefficients Γ . Limiting the number of echoes per branch means that we put an upper limit on i, j, k , and ℓ in (15).

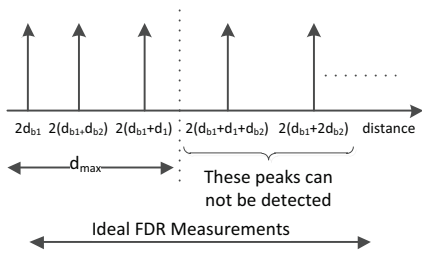


Fig. 5. Ideal FDR correlation and the effect of limited range.

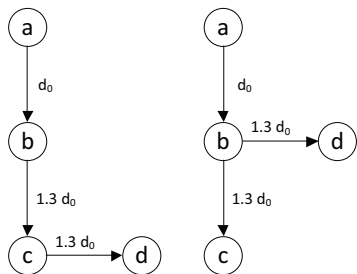


Fig. 6. Example of ambiguity.

C. Distance Limitation

To move one step further towards the practical case, the measurements are limited to a maximum distance d_{\max} . This assumption is realistic, since the signal suffers attenuation that increases with the distance traveled. d_{\max} depends on the sensitivity of the receiver. Fig. 5 shows the effect of the maximum distance on the FDR correlation. This limitation will lead to an increase of the number of the possible topologies that are consistent with the measured FDR correlation and need to be processed by the algorithm described below. The extreme case will be that only the first peak is within distance d_{\max} . Then, any topology having the first branch of length d_{b1} is a possible topology. As d_{\max} increases the number of possible topologies decreases.

D. Cases of Ambiguity

Even if we have access to the ideal FDR correlation, in some cases, we can find more than one topology that is consistent with it. Figure 6 shows an example of two topologies that generate the same ideal FDR correlation. To resolve such ambiguity, some prior information is required. Another solution is to make use of the magnitude and phase information in the trace to exclude some of the possibilities.

E. The Algorithm

We are now ready to introduce the algorithm for topology inference. The pseudo-code for the proposed algorithm is given in Fig. 7. It reconstructs the topology using a step-by-step approach; that is, the peaks in the measured FDR correlation are processed one-by-one. For each of the possible topologies, a new node is connected to an existing node to form a set of candidate topologies. The FDR correlation $y(d)$ is then generated for each candidate topology. If it is consistent

Input is the FDR measurement $y(d)$ with N_{peak} peak locations.
Initialize \mathcal{S} , the set of possible topologies, with a two-node topology.
For $i = 1, \dots, N_{\text{peaks}}$
1) For $j = 1, \dots, |\mathcal{S}|$:
2) Load the topology T_j from \mathcal{S} with the number of nodes N_{nodes} .
3) If peak number i is consistent with T_j keep T_j in \mathcal{S} .
4) For $k = 1, \dots, N_{\text{nodes}}$:
5) Add a new node connected to node number k , with the proper distance.
6) Generate the FDR correlation for the new topology.
7) If the generated correlation is consistent with $y(d)$, the topology is added to \mathcal{S} , and steps 4 and 5 are repeated unless already N_{\max} new nodes connected.

Fig. 7. The Proposed algorithm.

with the measured FDR correlation, then the topology is added to the set of possible topologies. In some cases, we may need to add more than one node for the same peak location (e.g. the case of equal branches connected to the same point as for node 'b' at the right-hand side in Fig. 6). We consider a maximum number of nodes to be added at one step of N_{\max} .

IV. SIMULATION RESULTS

For the previously mentioned graph approach, the results will be presented for two experiments. For the first experiment, the algorithm is tested for a topology of 10 nodes. In the second experiment, we consider a group of randomly generated topologies each consisting of 6 nodes, and the effect of d_{\max} is studied. For both experiments, the ideal correlation was simulated using (15). The maximum number of echoes per branch was limited to 3. We chose $N_{\max} = 2$ for the detection step, i.e., the algorithm can not detect topologies with more than two equal branches connected to the same branch point.

A. Results for Experiment 1

For this experiment, we simulated the correlation for a topology of 10 nodes. Naming the nodes from '1' to '10', and writing distances as multiples of some reference distance d_0 , the adjacency list for this topology is given by

$$L = \begin{bmatrix} 1 & 2 & 2 & 2 & 3 & 3 & 7 & 7 & 7 \\ 2 & 3 & 4 & 5 & 6 & 7 & 8 & 9 & 10 \\ 2.5 & 2.6 & 5.2 & 5.2 & 5.8 & 6.3 & 7.1 & 7.2 & 10.7 \end{bmatrix}^T.$$

where $(\cdot)^T$ represents the transpose of the matrix.

Running our algorithm to reconstruct the topology using a sufficiently large d_{\max} to account for all peaks returned the correct topology.

B. Simulation Setup and Results for Experiment 2

For this experiment, the adjacency list was randomly generated for 1000 different topologies each consisting of 6 nodes. The distance was chosen for each connection as $d_i = k_i d_0$, where k_i is generated randomly according to a uniform distribution over $[1, 11]$. d_0 is a scaling factor to adjust the distance according to the available resolution. Without loss of generality, $d_0 = 1$ for this experiment. d_i was approximated

TABLE I
SIMULATIONS RESULTS FOR EXPERIMENT 2.

N_{eff} (%)	10	15	20	35	50	55	75	90
r (%)	47	7	2.7	0.7	0.4	0.1	0	0
a (%)	47	26	9.9	1.4	1.9	1.3	1.2	1.1

to two decimal places to allow for the possibility of ambiguity (i.e., the probability of equal branches). The node-indices in the first two columns of the adjacency list were randomly generated according to a uniform discrete distribution from the set $\{1, 2, \dots, 6\}$. We assumed topologies with no loops. Instead of fixing d_{max} for all of the topologies, a limitation was made on N_{eff} , which is the maximum number of the peaks in the correlation that can be detected, which leads to a variable value for d_{max} . This choice was made for fair comparison between different topologies, which experience different distance ranges. Also, since each peak adds new information that helps determine the right topology, the number of peaks is more important than the location of the peaks.

Table I shows the results for Experiment 2, averaged for the 1000 sample topologies. The first row represents N_{eff} as a percentage of the total number of peaks in the correlation. For example, 50 percent indicates that only half of the peaks were used to reconstruct the topology (recall that the number of peaks in the correlation is finite due to the assumption of limited number of echoes).

The results are evaluated according to two parameters as follows

- 1) The failure rate r , which represents the number of times the set of possible topologies exceeded a certain threshold. We should expect that as the threshold increases, r decreases. For this experiment the threshold is 350, i.e. if $|\mathcal{S}| > 350$, the algorithm will stop working on the current topology. In this case, the algorithm can detect the true topology, but the problem is in the size of the set of possible topologies which is deemed too large to be processed.
- 2) The ambiguity rate a , which represents the number of times where $|\mathcal{S}| > 1$ at the end of the execution of the algorithm (i.e. there is more than one possible topology). a was computed as a percentage of the successful runs only.

The results show that the algorithm can reconstruct the topology, even for small values of N_{eff} (short maximum distance). Also, as N_{eff} increases, both r and a decrease. This should be expected, since as d_{max} increases, more information about the topology is available and the algorithm can eliminate erroneous candidate topologies. The results in Table I are encouraging. Further steps are evaluation of convergence of the algorithm to a single topology, consideration of larger topologies and missing peaks in the FDR correlation due to attenuation, and experimental tests.

V. CONCLUSION

In this paper, we have proposed a technique for topology inference of power line networks. This technique is based on

the distance measurements obtained from FDR. Results show that even if the maximum detectable distance is limited, the algorithm can reconstruct the topology successfully. In some cases there may be more than one possible topology consistent with the measurements. However, the true topology is always one of these topologies.

REFERENCES

- [1] H. Ferreira, L. Lampe, J. Newbury, and T.G. Swart (Editors), *Power Line Communications: Theory and Applications for Narrowband and Broadband Communications over Power Lines*. John Wiley & Sons, Jun. 2010.
- [2] G. Bumiller, L. Lampe, and H. Hrasnica, "Power line communications for large-scale control and automation systems," *IEEE Commun. Mag.*, vol. 48, no. 4, pp. 106–113, Apr. 2010.
- [3] S. Galli, A. Scaglione, and Z. Wang, "For the grid and through the grid: The role of power line communications in the smart grid," *Proc. IEEE*, vol. 99, no. 6, pp. 998–2017, 2011.
- [4] L. Lampe, R. Schober, and S. Yiu, "Distributed space-time coding for multihop transmission in power line communication networks," *IEEE J. Sel. Areas Commun.*, vol. 24, no. 7, pp. 1389–1400, Jul. 2006.
- [5] A. M. Tonello, F. Versolatto, and S. D'Alessandro, "Opportunistic relaying in in-home PLC networks," in *IEEE Global Communications Conference (GlobeCom)*, Dec. 2010.
- [6] L. Lampe and A. Vinck, "On cooperative coding for narrowband PLC networks," *Int. J. Electron. Commun. (AEU)*, no. 8, pp. 681–687, Aug. 2011.
- [7] T. Sartenaer and P. Delogne, "Powerline cables modelling for broadband communications," in *Int. Symp. on PLC and Its Appl. (ISPLC)*, Apr. 2001.
- [8] D. Schneider, J. Speidel, L. Stadelmeier, and D. Schill, "Precoded spatial multiplexing MIMO for inhome power line communications," in *IEEE Global Commun. Conf. (GlobeCom)*, Nov.-Dec 2008.
- [9] M. Biagi and L. Lampe, "Location assisted routing techniques for power line communication in smart grids," in *IEEE International Conference on Smart Grid Communications (SmartGridComm)*, Oct. 2010.
- [10] T. Esmailian, F. Kschischang, and P. Gulak, "In-building power lines as high-speed communication channels: Channel characterization and a test channel ensemble," *International Journal of Communication Systems*, vol. 16, pp. 381–400, 2003.
- [11] T. Erseghe, F. Lorenzon, S. Tomasin, A. Costabeber, and P. Tenti, "Distance measurement over PLC for dynamic grid mapping of smart micro grids," in *IEEE International Conference on Smart Grid Communications (SmartGridComm)*, Oct. 2011.
- [12] S. Galli, , and K. Kerpez, "Single-ended loop make-up identification-part I: A method of analyzing TDR measurements," *IEEE Trans. Instrum. Meas.*, vol. 55, no. 55, pp. 528–537, 2006.
- [13] B. Celaya and D. Dodds, "Single-ended DSL line tester," in *Canadian Conf. on Electr. and Comp. Eng. (CCECE)*, vol. 4, May 2004, pp. 2155 – 2158.
- [14] D. E. Dodds, M. Shafique, and B. Celaya, "TDR and FDR identification of bad splices in telephone cables," in *Canadian Conf. on Electr. and Comp. Eng. (CCECE)*, May 2006, pp. 838 –841.
- [15] B. de la Torre, "DSL line tester using wideband frequency domain reflectometry," Master's thesis, University of Saskatchewan, 2004.
- [16] D. Dodds and B. Celaya, "Locating water ingress in telephone cables using frequency domain reflectometry," in *Canadian Conf. on Electr. and Comp. Eng. (CCECE)*, May 2005, pp. 324 –327.
- [17] D. Dodds, "Single-ended FDR to locate and specifically identify DSL loop impairments," in *IEEE Intl. Conf. Commun. (ICC)*, Jun. 2007, pp. 6413 –6418.